中國機械工程學刊第四十二卷第五期第 451~459 頁(民國一百一十年)
Journal of the Chinese Society of Mechanical Engineers, Vol.42, No.5, pp. 451~459 (2021)

Modified Inverse Algorithm for SAC305 Solder Joint Life Prediction

Ning Luo*, **, Ching-I Chen*, Hong Xing Qiu******

Keywords: SAC305, Life Prediction Model, Finite Element Method, Fatigue Index

ABSTRACT

To predict the lifetime of the SAC305 solder joint in thermal shock test and temperature cycling test, a suite of wafer-level chip-scale packages (WLCSPs) were investigated by experiments and finite element simulations. Due to the insufficient experimental life data provided by the manufacture, a three-step modified inverse algorithm is adopted. First, Sn95.5Ag3.8Cu0.7 solder joints were simulated, and the lifetime were evaluated to check the consistency between the experimental and simulated lifetimes. Second, discrepant life was modified by analyzing the correlations of the life fatigue indices in the finite element simulation, thus providing the absent experimental life data. Third, life prediction models of SAC305 Anand constitutive material were developed based on the accumulated creep strain energy density and accumulated creep strain. Finally, the SAC305 life prediction model was verified in a solder joint experiment on another WLCSP. The lifetimes obtained by the model and the new experiment differed within 8%.

INTRODUCTION

The semiconductor industry takes a leading position in modern technology. Miniaturized electronic devices with light weight, multifunctionality, and high integration have been increasingly demanded over the past two decades and packaging patterns have progressively evolved to satisfy electronic product and device requirements. Each generation of electronic packages has arisen from advanced technology contributions, but the reliability problems of packages should be considered in the early design stage.

The semiconductor industry is a complex multi-field technology requiring advanced material development and manufacture processes to produce well-functioning electronic components and devices. An electronic package consists of a printed circuit board (PCB), substrate, chip, under bump metal (UBM), dielectric layer, solder joints, underfill, and redistribution layers, which are vulnerable under environmental loading. Manufacturers have tried different methodologies to overcome the failure problem. Solder joints used for mechanical support and electrical signal transmission remain among the most important infrastructures in packaged devices. However, solder joints become less reliable as their number increases and their size diminishes. Solder joints in packaged devices can fail under thermal, mechanical, electrical, drop impact, or vibration loading conditions, or a combination of these conditions. Failures occur when loading exceeds the fracture strength of the components or when damage accumulates under alternating low-amplitude stress. The stresses and strains within packages under external thermal loading or thermomechanical-related failures caused by internal heating comprise approximately 65% of all failures (Zhang, et al, 2006).

According to the Joint Electron Device Engineering Council (JEDEC) standard, thermal loading is most investigated through temperature cycling tests (TCTs), thermal shock test (TSTs), and power cycling tests. In a thermal test, the coefficient of thermal expansion and stiffness mismatch between package assemblies induce thermal stresses and strains in the solder joints. The damage caused by these stresses and strains will accumulate and eventually lead to joint failure. This topic has been investigated by many scholars (Fan, et al, 2020; Chi, et al, 2019; Su, et al, 2020; Huang, et al, 2019).

Paper Received March, 2021. Revised June, 2021. Accepted August, 2021. Author for Correspondence: Ning Luo

* *Lecturer, School of Mechanical and Automotive Engineering, Xiamen University of Technology, Xiamen 361024, China*

** *Doctoral candidate, Ph. D. Program in Engineering Science, Chung Hua University, Hsinchu 30012, Taiwan*

*** *Professor, Department of Mechanical Engineering, Chung Hua University, Hsinchu 30012, Taiwan*

**** *Vice Director, R&D Institute, 3DFAMILY Technology Co., Ltd., New Taipei 23674, Taiwan*

To investigate failure in solder joints, the lifetime of solder joints can be predicted from their material properties in actual and numerical (finite element) experiments. Real experiments are usually performed by acceleration testing, which requires a long lead time to obtain the test data. The associated costs not only increase product development time but also constrain design optimization (Syed,2001). On the upside, acceleration testing does not require the provided material properties and can investigate other failure mechanisms that reduce the lifetime of solder joints through cracking and delamination of their intermetallic compounds (Li, 2019; Li and Sun, 2017; Galbiati, 2017). Furthermore, from an accuracy viewpoint, deriving a life prediction model from inelastic strain or energy density measurements in a tiny solder joint is impractical. With the continuous development of finite element technology, the lifetime of solder joints has increasingly been predicted through finite element methods (Chen, et al, 2018; Wang, et al, 2020; Chen, et al, 2021). Syed (Syed, 2001; Syed, 2006) pointed out two sources of errors in any finite element-based life prediction model: the finite element mesh and assumptions, and the material properties used in the constitutive model that describes the behavior of solder joints during temperature cycling.

Lead-free solder is used worldwide under the Waste from Electrical and Electronic Equipment and Restriction of Hazardous Substances directives for environmental protection. At present, SnAgCu (SAC) series alloys are the most popular solders owing to their satisfactory soldering performance, excellent creep resistance, and reliable thermal fatigue. Therefore, the mechanical behaviors of leadless solder joints are commonly reported (Qi, et al, 2006; Kim and Jung, 2007; Zhang, et al, 2013; Bhate, et al, 2008). The material parameters of different lead-free solders are given by Zhang (Zhang, et al, 2009).

The popular material constitutive models used in the microelectronics industry are the Anand model, the steady-state creep model, and the double power-law creep model. The fatigue lives and stress–strain responses of solders predicted by different models can be compared in simulations. The creep, elastic–plastic creep, and Anand models are most suitable for predicting fatigue life in thermal cycling simulations. However, the temperature- and time-dependent creep behaviors of SAC solders (e.g., SAC305, SAC405, and SAC387) are often modeled using the hyperbolic sine creep equation (Talledo, 2021).

Fatigue Life Models

The life prediction models proposed in the literature can be expressed in the following general form:

$$\mathrm{N}_f = \alpha (FI)^{\beta} \tag{1}$$

where N_f is the number of cycles to failure and FI is the fatigue index, which usually refers to the accumulated creep strain ε_{acc} or the total inelastic deformation energy density W_{cr} during one temperature cycle. The coefficients α and β can be determined by curve fitting to the life data obtained in experiments and the failure index derived from simulations.

Many solder joint life prediction models are developed based on experimental data and finite element simulation techniques (Schubert, et al, 2003; Zahn, 2003; Hsieh and Tzeng, 2014). The solder joint life prediction model of Syed (Syed, 2006) uses the constitutive equation of SAC405 published by Wiese (Wiese, et al, 2003). Creep behavior is modeled using a hyperbolic sine equation, and the life prediction models of the solder balls are given as

$$N_f = 3.5864 \Delta \varepsilon_{acc}^{-1.1198} \tag{2}$$

$$N_f = 144.93 \Delta W_{cr}^{\ -1} \tag{3}$$

where $\Delta\varepsilon_{acc}$ and ΔW_{cr} are the accumulated creep strain and the creep strain energy density, respectively, over the last temperature cycle. In experiments and simulations, Schubert (Schubert, et al, 2003) evaluated the fatigue life models of Sn95.5Ag3.8Cu0.7 solder balls in different package types. The life prediction models are given as

$$N_f = 4.5 \Delta \varepsilon_{acc}^{-1.295} \tag{4}$$

$$N_f = 345 \Delta W_{cr}^{-1.02} \tag{5}$$

Zahn (Zahn, 2003) predicted the lifetime of 95.5Sn4Ag5Cu solder balls using the following equation:

$$N_f = 2083 \Delta W_{inelastic}^{-0.1204} \tag{6}$$

where $\Delta W_{inelastic}$ is the nonlinear change in strain energy density during the last cyclic load, which includes the creep strain energy density and the plastic strain energy density. The Garofalo–Arrhenius creep model of SAC105 is given by Hsien (Hsieh and Tzeng, 2014)

$$N_f = 27612 (\Delta W)^{-2.2635} \tag{7}$$

$$N_f = 3.2661 (\Delta \gamma)^{-3.2075} \tag{8}$$

where ΔW and $\Delta\gamma$ are the changes in creep strain energy density and equivalent creep strain during one cycle, respectively.

Most researchers select one of the life prediction models given by equations. (2) – (8) by assuming similar compositions of the SAC series. Alternatively, they investigate life tendency by comparing fatigue indices such as creep strain energy density and accumulated creep strain. However, these approaches exclude the life prediction of SAC305. Xiao (Xiao, et al, 2014) predicted the lifetime of the SAC series using the finite element method. They investigated the reliability of solder joints in a chip-scale package device mounted on a printed circuit board. The Anand model of Sn3.0Ag0.5Cu solder was consistent with the life prediction model of Sn95.5Ag3.8Cu0.7.

In this paper, the fatigue life of SAC305 is investigated in a suite of wafer-level chip-scale packages (WLCSPs). Usually, experimental life data can be curve-fitted using fatigue indices to derive the life model. As life data in TSTs and TCTs provided by the manufacturer were insufficient, they were evaluated here in a three-step modified inverse algorithm. First, a Sn95.5Ag3.8Cu0.7 solder joint under TST and TCT conditions was modeled using Eqs. (4) and (5) in a finite element simulation, and the obtained lifetime was compared with that obtained in a real experiment. Second, discrepant life was modified by analyzing the correlation of life fatigue indices obtained in finite element simulation, thus providing the absent experimental life data (here called the simulated experimental life). Third, life prediction models of SAC305 Anand constitutive material were developed with curve fitting of the fatigue indices by finite element simulation. Finally, the experimental life of the solder joint was evaluated in another package to verify the derived life prediction model of SAC305. The experimental and simulated lives differed within 8%.

EXPERIMENTAL LIFE

Following the JEDEC standard, thermal cycling tests were conducted on a set of WLCSP packages provided by the manufacturer. In the TST, the temperature was raised from −25 °C to 125 °C at a ramp rate of 150 °C/min and a dwell time of 9 min at peak temperature (giving a whole cycle time of 20 min). In the TCT, the temperature was raised from −40 °C to 125 °C at a frequency of 60 min per cycle, with dwell and ramp times of 15 min each.

Table 1. Experimental lives of the packages in the thermal cycling test

Package No.	Package thickness (mm)	Characteristic life	
		TST	TCT
A (1)	0.400	2000	×
A (2)	0.550	1642	×
A (3)	0.715	1200	×
A (4)	0.815	950	×
B	0.400	×	1250

The diameter and pitch of the solder balls in the WLCSPs are 0.31 and 0.5 mm, respectively. According to the number and distribution of solder joints, the packages are divided into two modules. Each of the four packages in module A contains 112 solder joints distributed in a peripheral array. Module B contains one package with 256 solder joints distributed in a global array. The TSTs and TCT were conducted on the four packages in module A and the single package in module B, respectively. Characteristic life was determined as the number of cycles at which more than 63.2 % of solder joints in the package failed. The experimental lives are shown in Table 1.

FINITE ELEMENT MODELING

When experimental life is sufficiently provided, a life model can be obtained by curve fitting the fatigue indices from the finite element simulations. The main aim is to fill the absent life entries in Table 1. This can be achieved by applying the constitutive life model of the Sn95.5Ag3.8Cu0.7 material in literature (Zahn, 2003). The life difference between the finite element method and the experiment can be attributed to the different SAC materials. Modified equations (4) and (5) reduce the life difference in the previous step and provide the absent lives.

In the finite element model, the chip length and PCB thickness were 6.0 and 0.8 mm, respectively, in module A and 8.0 and 1.0 mm, respectively, in module B. Figure 1 is a cross-sectional view of the package in the soldered part. Table 2 lists the material properties of the components in the packages. The Young's modulus of the Sn95.5Ag3.8Cu0.7 solder joint is given by

$$E = 61251 - 58.5T \tag{9}$$

where T is absolute temperature (K).

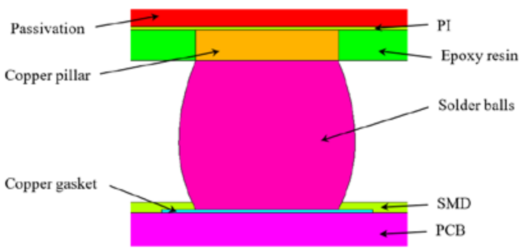

Figure 1. Cross-sectional view of the package in the solder part

Table 2. Material properties of the WLCSP components

Component	E (MPa)	α	v (ppm/°C)
Chip	131000	0.28	2.6
Passivation	314000	0.33	4
Epoxy resin	14000	0.34	20
Copper	117000	0.34	16.7
Solder mask	−25@6000	0.35	0.35

	22@4100 70@1420 100@330 150@100		
PCB	EX = 25420 EY = 11000 EZ = 25420 GXY = 4970 GYZ = 4970 GXZ = 11450	NUXY= 0.39 NUYZ = 0.39 NUXZ = 0.11	ALPX = 14 ALPY = 45 ALPZ = 14
Solder joint	61251-58.5T	0.36	20

The steady-state creep behavior of the solder joints was modeled using the generalized Garofalo–Arrhenius constitutive equation:

$$\dot{\varepsilon}_{cr} = C_1(\sinh(C_2\sigma))^{C_3} e^{\frac{-C4}{T}} \qquad (10)$$

where $\dot{\varepsilon}_{cr}$ is the steady-state creep strain rate and σ is the stress. The values of the constants C_1, C_2, C_3, and C_4 are 277984 s^{-1}, 0.02447 mm^2/N, 6.41, and 6500 K, respectively.

Figure 2 shows the three-dimensional quarter finite element models of modules A and B. Thermal cycling loads were simulated in TSTs or TCTs under real experimental conditions.

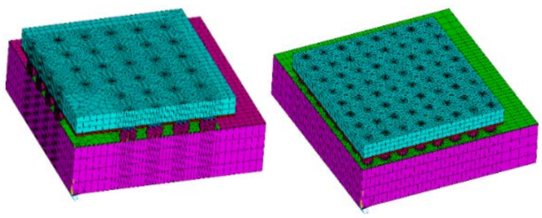

Module A Module B

Figure 2. Finite element models of the two modules

Figures 3 and 4 show the von Mises creep strain and the creep strain energy density of package A (1), respectively. The von Mises creep strain was maximized on the solder joint adjacent to the solder joint farthest from the center, and the creep strain energy density was maximized on the solder joint farthest from the center. The same conclusions were drawn in the simulations of the other packages. Without loss of generality, the fatigue index was therefore determined at the solder joint farthest from the center.

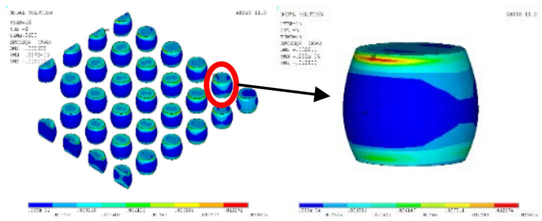

Figure 3. Von Mises creep strain distribution in package A (1)

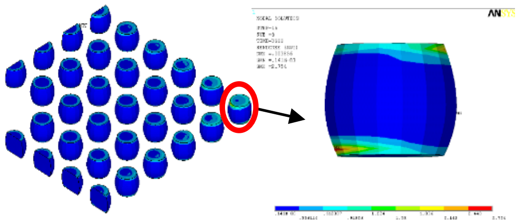

Figure 4. Creep strain energy density distribution in package A (1)

RESULTS AND DISSCUTION

The fatigue failure indices (accumulated creep strain and energy density) of the 25-μm-thick layers of solder joints were calculated using the volume averaging technique. The accumulated creep strains and creep energy densities, provided as standard outputs from ANSYS, could be volume-averaged by simple postprocessing steps. The accumulated creep strain energy densities (ΔW) and accumulated von Mises creep strains ($\Delta\varepsilon$) of the five packages in the third TST cycle are shown in Table 3. Equivalent values in the third TCT cycle are given in Table 4.

Table 3. Fatigue indices during the third TST cycles

Package	ΔW	$\Delta\varepsilon$	log(ΔW)	log($\Delta\varepsilon$)
A (1)	0.2115	0.0075	−0.6748	−2.1255
A (2)	0.3373	0.0113	−0.4720	−1.9489
A (3)	0.4971	0.0157	−0.3036	−1.8036
A (4)	0.5877	0.0182	−0.2308	−1.7411
B	0.2835	0.0098	−0.5474	−2.0083

Table 4. Fatigue indices during the third TCT cycles

Package	ΔW	Δε	log(ΔW)	log(Δε)
A (1)	0.1894	0.0086	−0.7226	−2.0635
A (2)	0.29944	0.0128	−0.5237	−1.8925
A (3)	0.42995	0.0177	−0.3666	−1.7518
A (4)	0.50580	0.0204	−0.2960	−1.6914
B	0.25141	0.01117	−0.5996	−1.9520

The logarithmic form of Eq. (1) expresses the predicted life N_f as a linear function of the fatigue index. In other words, log($\Delta\varepsilon$) is linearly related to log(ΔW) as shown in Figure 5. Clearly, the log($\Delta\varepsilon$) versus log(ΔW) plots of TST and TCT were parallel, showing that the two thermal loads were closely related and differed only by their temperature loading. By contrast, the accumulated von Mises creep strain ($\Delta\varepsilon$) and accumulated creep strain energy density (ΔW) were higher and lower, respectively, in the TCT than in the TST.

Tables 5 and 6 list the lives evaluated by Eqs. (4) and (5) in the TST and TCT, respectively. The differences between the results of the two equations reached 40% in the TST and 20% in the TCT. These discrepancies were mainly attributable to the differences among the SAC materials. The lifetime of module B in the TST (1796 and 1248 based on the accumulated creep strain and creep energy density, respectively) cannot be predicted by Eqs. (4) and (5) because the lifetime varies widely among the solder joints in module A. Conversely, the absent lives of module A in the TCT cannot be predicted by Eqs. (4) and (5) because only one life datum is available in module B.

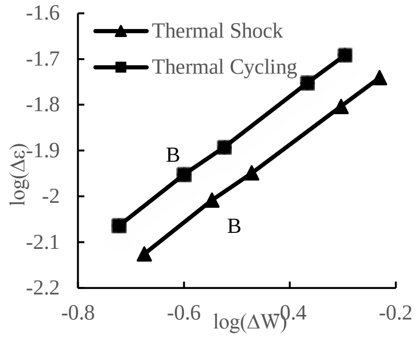

Figure 5. Relationship between log ($\Delta\varepsilon$) and log (ΔW)

Table 5. Predicted lives of the solder joints in the TST

	Module A				Module B
	1	2	3	4	
$N_f = 4.5\Delta\varepsilon_{acc}^{-1.295}$	2546 (+27.3%)	1503 (−8.46%)	975 (−18.75%)	809 (−14.84%)	1796
$N_f = 345\Delta W_{cr}^{-1.02}$	1683 (−15.85%)	1045 (−36.35%)	704 (−41.33%)	593 (−37.58%)	1248
Experimental life	2000	1642	1200	950	×

Table 6. Predicted lives of the solder joints in the TCT

	Module A				Module B
	1	2	3	4	
$N_f = 4.5\Delta\varepsilon_{acc}^{-1.295}$	2117	1271	835	698	1516 (+21.28%)
$N_f = 345\Delta W_{cr}^{-1.02}$	1883	1180	816	691	1411 (+12.88%)
Experimental life	×	×	×	×	1250

Simulated Experimental Life

Using the fatigue indices and experiment lives of module A in the TST, the life prediction models of Eqs. (4) and (5) were modified by fitting the data with the least-squares linear regression method. The modified expressions are given by Eqs. (11) and (12), respectively:

$$N_f = 701.5\Delta W^{-0.7073} \tag{11}$$

$$N_f = 38.78\Delta\varepsilon^{-0.81622} \tag{12}$$

As shown in Table 7, the modified predicted lives of the solder joints in module A differed within 8%. The fatigue indices of module B were located on the $\Delta\varepsilon$ versus ΔW line of module A (see Figure 5). The average predicted lives of module B (1711 and 1690 based on the accumulated creep energy density and creep strain, respectively) may be regarded as the simulated experimental life (1700; see Table 7).

Table 7. Modified predicted lives in the TST

	Module A				Module B
	1	2	3	4	
$N_f = 701.5\Delta W^{-0.7073}$	2105 (+5.25%)	1513 (−7.86%)	1150 (−4.17%)	1022 (+7.58%)	1711
$N_f = 38.78\Delta\varepsilon^{-0.81622}$	2106 (+5.3%)	1511 (−8%)	1150 (−4.2%)	1023 (+7.7%)	1690
Experimental life	2000	1642	1200	950	×
Simulated experimental life	×	×	×	×	1700

The situation differs in the TCT because module B contains only one package. As the log ($\Delta\varepsilon$) versus log (ΔW) plots in the TST and TCT are parallel, the relationship between log (N_f) and log ($\Delta\varepsilon$), and the relationship between log (N_f) and log (ΔW) should be parallel. By assuming a constant exponential β in Eqs. (11) and (12), the TCT life prediction models were derived from the experiment life data in module B, and they are given by

$$N_f = 470.7\Delta W^{-0.7073} \tag{13}$$

$$N_f = 31.9\Delta\varepsilon^{-0.81622} \tag{14}$$

Table 8 lists the modified predicted lives in module A. As shown in Figure 5, the fatigue index of module B is located on the $\Delta\varepsilon$ versus ΔW line of module A. The average predicted lives in each package of module A, determined by Eqs. (13) and (14), can be regarded as the simulated experimental life in that package (see Table 8).

Table 8. Modified predicted lives in the TCT

	Module A				Module B
	1	2	3	4	
$N_f = 470.7\Delta W^{-0.7073}$	1527	1105	855	762	1250
$N_f = 31.9\Delta\varepsilon^{-0.81622}$	1542	1117	858	766	1250
Experimental life	×	×	×	×	1250
Simulated experimental life	1535	1111	857	764	×

Life Prediction Model of SAC305 Solder Joint

The solder joint material was replaced with the Anand constitutive material of SAC305 (Motalab,2012), and the simulations were repeated. From the experimental results and the simulated fatigue-index data, the life prediction models of the SAC305 solder joint were deduced.

The Anand model constants derived from the stress–strain data are listed in Table 9. The thermal expansion coefficient of SAC305 is 24.7 (ppm/°C), the Poisson's ratio is 0.4, and the Young's modulus is the following function of temperature T (°C):

$$E(T) = 42.125 - 0.15T \text{ (GPa)} \tag{15}$$

Table 9. Anand model parameters of SAC305 solder joints

Constant Number	Anand Constant	Units	SAC305 (Stress–Strain)
1	s_0	MPa	21
2	Q/R	1/K	9320
3	A	s^{-1}	3501
4	ξ	-	4
5	m	-	0.25
6	h_o	MPa	180000
7	$\hat{S}$	MPa	30.2
8	n	-	0.01
9	a	-	1.78

The fatigue index and accumulated creep strain energy density (ΔW) of each package in the TSTs and TCTs are given in Tables 10 and 11, respectively. The life predictions of Eq. (11) and (13) differed by up to 14% in the TST and 20% in the TCT. The fatigue indices obtained in the life prediction of SAC305 are inapplicable to Eqs. (11) and (13), which are based on the Sn95.5Ag3.8Cu0.7 constitutive material. By the same reason, the fatigue indices of the SAC305 experimental life prediction are inapplicable to Sn95.5Ag3.8Cu0.7 as discussed above. The life prediction models of SAC305 can be obtained by curve fitting of the fatigue indices obtained in the finite element model in this section and the life model in the previous section. The life prediction models in the

TST and TCT were obtained as Eqs. (16) and (17), respectively. Their results differed by 7% in the TST (Table 10) and 2% in the TCT (Table 11).

$$N_f = 683.2\Delta W^{-0.8117} \quad \text{(TST)} \qquad (16)$$

$$N_f = 515\Delta W^{-0.7958} \quad \text{(TCT)} \qquad (17)$$

Table 10. Life prediction model of SAC305 in the TST

	Module A				Module B
	1	2	3	4	
ΔW	0.25162	0.36889	0.52577	0.61668	0.33083
$N_f = 701.5\Delta W^{-0.7073}$	1862 (−6.92%)	1420 (−13.51%)	1105 (−7.89%)	987 (3.94%)	1534 (−9.77%)
$N_f = 683.2\Delta W^{-0.8117}$	2094 (4.70%)	1535 (−6.51%)	1151 (−4.05%)	1012 (6.48%)	1677 (−1.36%)
Experimental life	2000	1642	1200	950	×
Simulated experimental life	×	×	×	×	1700

Table 11. Life prediction model of SAC305 in the TCT

	Module A				Module B
	1	2	3	4	
ΔW	0.25591	0.37444	0.52732	0.61371	0.33111
$N_f = 470.7\Delta W^{-0.7073}$	1234 (−19.59%)	943 (−15.13%)	740 (−13.63%)	665 (−12.98%)	1029 (−17.71%)
$N_f = 515\Delta W^{-0.7958}$	1524 (−0.73%)	1126 (1.31%)	857 (0%)	760 (−0.57%)	1241 (−0.70%)
Experimental life	×	×	×	×	1250
Simulated experimental life	1535	1111	857	764	×

Verification

The SAC305 solder joint life prediction model in the TCT was verified in a WLCSP package with a through silicon via (TSV). In the TCT, temperature was raised from −40 °C to 85 °C at a frequency of 60 min per cycle, and the dwell and ramp times were 15 min each. The characteristic life was 2000.

The overall package, including the PCB, had a size of (6.534 × 5.724 × 1.555) mm^3, chip thickness was 0.095 mm, and the number of solder joints was 87. Package thickness was 0.563 mm. The diameter and pitch of the solder joints were 0.415 and 0.610 mm, respectively. The finite element model of the package is shown in Figure 6.

In the simulation, the accumulated creep strain energy density ΔW of the solder joints was calculated as 0.2016, and the lifetime (estimated by Eq. (17)) was 1842 (a difference of −7.9% from 2000). The difference possibly arises from the different temperature ranges and package types.

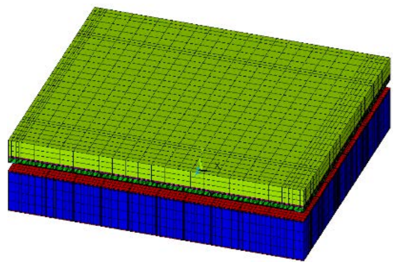

Figure 6. Finite element model of the WLCSP package with TSV

CONCLUSIONS

The fatigue life of the constitutive SAC305 Anand material was estimated from the experimental data of four WLCSPs with different thicknesses (0.40, 0.55, 0.715, and 0.815 mm) under thermal shock (module A) and a single package of thickness 0.4 mm under thermal cycling (module B). To complete the missing data, a modified inverse algorithm was run through the following steps:

(1) Verify Schubert's constitutive and life prediction models of the Sn95.5Ag3.8Cu0.7 material in comparison with experimental life data.
(2) Modify Schubert's life prediction model to predict the absent experiment life data.
(3) Obtain the life prediction model of SAC305 Anand based on the accumulated creep strain energy density change (ΔW) obtained in the TST and TCT.

Finally, the experimental life of the solder joints in another package was estimated using the derived SAC305 life prediction model. The experimental and simulation results differed within 8%.

ACKNOWLEDGMENTS

This research was supported by the Education and Science Research Projects of Young and Middle-Aged Teachers in Fujian Province, China (No. JAT190660)

REFERENCES

Bhate, D., Chan, D., Subbarayan, G., Chiu, C., Gupta, V. and Edwards, D. R., "Constitutive behavior of Sn3.8Ag0.7Cu and Sn1.0Ag0.5Cu alloys at creep and low strain rate regimes," Transactions on Components and Packaging Technologies. Vol.31, No. 3, pp. 622–633. (2008).

Chen, Z., Zhang, X., Lim, S., Lim, S., and Andriani, Y., "Solder Joint Reliability Simulation of Fan-out Wafer Level Package (FOWLP) Considering Viscoelastic Material Properties," Proc., of 2018 IEEE 20th Electronics Packaging Technology Conference (EPTC), Singapore, pp. 573-579. (2018).

Chen, Y., Jing, B., Li, J., Jiao, X., Hu, J. and Wang, Y., "Failure Analysis and Modeling of Solder Joints in BGA Packaged Electronic Chips," Transactions on Components, Packaging and Manufacturing Technology, Vol. 11, pp. 43-50. (2021).

Chi, G., Chen, I. and Liao, A., "Development of TCT Life Prediction Model of Solder for Power Module," Proc., of PCIM Euro 2019, Nuremberg, Germany, pp. 1-6. (2019).

Fan, H., Boettcher, T., Li, C., Cheam, E., Yang J., and Chen, H., "Solder Crack Improvement for A Power Package During TCT and PTC by Simulation," Proc. of EuroSimE2020, Cracow, Poland, pp. 1-4. (2020).

Galbiati, E., "Reliability evaluation of solder joints in electronics assemblies", Proc., of 2017 21st European Microelectronics and Packaging Conference & Exhibition, Warsaw, Poland, pp.1-5. (2017).

Hsieh, C. M. and Tzeng, S.L., "Solder Joint Fatigue Life Prediction in Large Size and Low-Cost Wafer-Level Chip Scale Packages", Proc., of 2014 15th International Conference on Electronic Packaging Technology, Chengdu, China. pp. 496-501. (2014).

Huang, Y., Luo, Y., Xiao F. and Liu, B., "Failure Mechanism of Die-Attach Solder Joints in IGBT Modules Under Pulse High-Current Power Cycling," Journal of Emerging and Selected Topics in Power Electronics, Vol. 7, No. 1, pp. 99-107. (2019)

Kim, J. W., Jung, S. B., "Design of solder joint structure for flip chip package with an optimized shear test method," Journal of Electronic Materials. Vol. 36, No. 6, pp. 690–696. (2007).

Li, W.M., "An analysis case on the crack failure of CBGA solder joints", Proc., of 2019 20th International Conference on Electronic Packaging Technology, Hong Kong, China, pp.1-4. (2019).

Li, W.M., and Sun, X.W., "An analysis case on the failure of BGA solder joints", Proc., of 2017 18th International Conference on Electronic Packaging Technology, Harbin, China, pp.731-734. (2017).

Motalab, M., Cai, Z., Suhling J. C. and Lall, P., "Determination of Anand constants for SAC solders using stress-strain or creep data," Proc., of 13th InterSociety Conference on Thermal and Thermomechanical Phenomena in Electronic Systems, San Diego, USA, pp. 910-922. (2012).

Qi, Y., Ghorbani, H.R., Spelt, J.K., "Thermal fatigue of SnPb and SAC resistor joints: analysis of stress-strain as a function of cycle parameters," Transactions on Advanced Packaging, Vol. 29, No. 4, pp. 690–700. (2006).

Schubert, A., Dudek, R., Auerswald, E., Gollbardt, A., Michel, B. and Reichl, H., "Fatigue life models for SnAgCu and SnPb solder joints evaluated by experiments and simulation," Proc., of 53rd Electronic Components and Technology Conference, New Orleans, USA, pp. 603-610. (2003).

Su, D., Zhao, D., Zhang, L., Yang, H., Wang C. and Jiang, W., "Reliability assessment of flip chip interconnect electronic packaging under thermal shocks," Proc., of 2020 21st International Conference on Electronic Packaging Technology, Guangzhou, China, pp. 1-4. (2020).

Syed, A., "Predicting solder joint reliability for thermal, power, and bend cycle within 25% accuracy," Proc., of 51st Electronic Components and Technology Conference, Orlando, USA. (2001).

Syed, A., "Updated Life Prediction Models for Solder Joints with Removal of Modeling Assumptions and Effect of Constitutive Equations," EuroSime 2006, Como, Italy, pp. 1-9. (2006).

Talledo, J., "Modeling Study on the Solder Joint Reliability of a Leadframe Package under

Powered Thermal Cycling," Journal of Engineering Research and Reports, Vol. 20, No. 3, pp. 37-43. (2021).

Wang, J., Xue, S., Wang, J., et al. "Comparative study on the reliability of SnPbSb solder joint under common thermal cycling and extreme thermal shocking", Journal of Materials Science: Materials in Electronics, Vol.31, pp. 5731-5737. (2020).

Wiese, S., Meusel, E. and Wolter, K., "Microstructural dependence of constitutive properties of eutectic SnAg and SnAgCu solders," Proc., of 53rd Electronic Components and Technology Conference, New Orleans, LA, USA, pp. 197-206. (2003).

Xiao, H., Luo D. J., and Zou, Y. B., "Damage Behavior and Life Prediction for Lead-Free Solder Joints in a CSP Assembly under Thermal Cycling," Proc., of 2014 10th International Conference on Reliability, Maintainability and Safety (ICRMS). Guangzhou, China. pp. 650-654. (2014).

Zahn, B. A., "Solder joint fatigue life model methodology for 63Sn37Pb and 95.5Sn4Ag0.5Cu materials," Proc., of 53rd Electronic Components and Technology Conference, New Orleans, USA, pp. 83-94. (2003).

Zhang, G. Q., Driel, W. D. van, and Fan, X. J., "Mechanics of Microelectronics", Springer: Dordrecht. The Netherlands, pp. 35–63. (2006).

Zhang, L., Han, J.G., He, C.W. and Guo, Y.H., "Reliability behavior of lead-free solder joints in electronic components," Journal of materials science. Vol. 24, No. 1, pp.172–190. (2013).

Zhang, L., Xue, S.B., Gao, L.L., Zeng, G., Chen, Y., Yu, S.L. and Sheng, Z., "Creep behavior of SnAgCu solders with rare earth Ce doping," Transactions of Nonferrous Metals Society of China, Vol. 19, No. 6, pp. 753–778. (2009).

修正逆演算法的 SAC305 錫球壽命預測

羅寧
廈門理工学院機械與汽車工程學院
中華大學工程科学博士学位学程

陳精一
中華大學機械工程系

邱弘興
智泰科技股份有限公司

摘要

為預測 SAC305 錫球在熱衝擊測試和溫度迴圈測試中的壽命，本文對一套晶圓級晶片尺寸封裝進行了實驗和有限元模擬研究。由於製造商提供的實驗壽命資料不足，因此採用了一種包含三個步驟的修正逆演算法進行推導。首先，在有限元模擬中評估了 Sn95.5Ag3.8Cu0.7 錫球的壽命，以檢查實驗壽命和模擬壽命之間的一致性。其次，通過分析有限元模擬中壽命疲勞指數的相關性來修正差異壽命，從而提供所缺乏的實驗壽命資料。第三，基於累積蠕變應變能量密度和累積蠕變應變，建立了 SAC305 Anand 材料屬性下的壽命預測模型。最后，SAC305 寿命预测模型在另一个晶圓級晶片尺寸封裝上的錫球实验中得到验证，模型壽命和新實驗獲得的壽命相差在 8% 以內。